

## Estimation of erosion and deposition by Unit Stream Power Erosion and Deposition in a sub-basin on the Mogi Guaçu River's margins, municipality of Mogi Guaçu, SP, Brazil

*Estimativa da erosão e deposição pela Unit Stream Power Erosion and Deposition em uma sub-bacia às margens do Rio Mogi Guaçu, município de Mogi Guaçu, São Paulo, Brasil*

Anna Hofmann Oliveira<sup>1</sup> , Gustavo Klinke Neto<sup>2</sup> , Sueli Yoshinaga Pereira<sup>2</sup> 

<sup>1</sup>Universidade Federal de São Carlos - UFSCar, Rodovia Anhanguera, km 174, SP-330, CEP 13600-970, Caixa Postal 153, Araras, SP, BR (annahofmann@ufscar.br)

<sup>2</sup>Universidade Estadual de Campinas - UNICAMP, Campinas, SP, BR (gus.klinke@gmail.com; sueliyos@ige.unicamp.br)

Received on July 23, 2020; accepted on January 6, 2022.

### Abstract

Information regarding the soil erosive processes that comprise the detachment, transport and deposition, are essential when analyzing hydrological processes associated with the generation of the flow in the landscape and water recharge. The USPED (Unit Stream Power Erosion and Deposition) model has been applied in several regions around the world for providing more accurate estimates, since it adds a physical base that relates the relief morphology with the erosion-defining runoff parameters. The current study aims to analyze erosion and deposition using the USPED model in a sub-basin on Mogi Guaçu River's margins, municipality of Mogi Guaçu, SP, Brazil, and generate subsidies for future diagnoses regarding areas in the region with greater capacity for water storage, based on less erosion. The loss of mineral and organic particles arising from the erosive process changes the soil's effective depth, texture and structure, directly and negatively impacting its capacity to absorb and retain water. 60% of the sub-basin's area was unaffected by considerable processes of erosion and deposition, both due to the current arboreal vegetation, but also the smooth relief of the site. The erosion and deposition sites have totaled 23.42 and 15.76% of the sub-basin area respectively, being adjacent to one another and preferably near or within the drainage network. The results of the spatialization were validated by the Kappa Index and revealed that the USPED model obtained an excellent agreement with the "ground truth". Stability in terms of erosion, favors the water recharge in area, since the soils present a sandy texture and in addition, the Latossolos, which make up 63% of the sub-basin, are deep and possess a high water storage capacity and permeability.

**Keywords:** Semi-empirical modeling; Surface runoff; Contribution area; Unit Stream Power Erosion and Deposition.

### Resumo

Informações a respeito dos processos erosivos do solo, que compreendem desagregação, transporte e deposição, são essenciais quando se deseja analisar processos hidrológicos associados à geração do escoamento na paisagem e à recarga de aquíferos. O modelo *Unit Stream Power Erosion and Deposition* (USPED) vem sendo aplicado em diversas regiões do mundo por oferecer estimativas mais precisas, uma vez que agrega uma base física que relaciona morfologia do relevo e parâmetros de escoamento definidores da erosão. O presente trabalho visa analisar a erosão e a deposição utilizando o modelo USPED em uma sub-bacia hidrográfica da planície aluvionar do Rio Mogi Guaçu, município de Mogi Guaçu, São Paulo, Brasil, e gerar subsídios para futuros diagnósticos de áreas com maior capacidade para armazenamento de água na região, baseado na menor erosão. A remoção de partículas minerais e orgânicas do solo, decorrente do processo erosivo, altera a profundidade efetiva, a textura, a estrutura e, conseqüentemente, interfere direta e negativamente em sua capacidade de absorver e reter água. A sub-bacia apresentou cerca de 60% de sua área não afetada por processos de erosão e deposição consideráveis, graças à vegetação arbórea atual, mas também ao relevo suave do local. Os locais de erosão e deposição totalizaram 23,42 e 15,76%, respectivamente, da área da sub-bacia, sendo adjacentes um ao outro e preferencialmente próximos ou dentro da rede de drenagem. Os resultados da espacialização foram validados pelo índice Kappa e revelaram que o modelo USPED obteve excelente concordância com a "verdade de campo". A estabilidade em termos de erosão favorece a recarga da água na área, uma vez que os solos apresentam textura arenosa e, além disso, os Latossolos, que compõem 63% da sub-bacia, são profundos e possuem alta capacidade de armazenamento e permeabilidade.

**Palavras-chave:** Modelagem semiempírica; Escoamento superficial; Área de contribuição; *Unit Stream Power Erosion and Deposition*.

## INTRODUCTION

The hydrographic basin is an open natural system whose processes are interlinked and in equilibrium, so that when analyzing the soil erosive process, it becomes relevant not only regarding the level of degradation to which an area is subjected, but also in the delineation of part of the hydrological phenomenon itself. From this perspective, the water dynamics on and within the landscape, with respect to surface runoff and infiltration, respectively, allow us to infer about the potential of water recharge in each region. Increased erosion may result from increased runoff and lead to lower recharge of aquifers, reducing base flow and increasing maximum outflows of watercourses. The reverse process will occur if there is increased infiltration (Nearing et al., 2011; Cecílio et al., 2013). In this sense, the understanding of the mechanisms that are related directly or indirectly with the erosion process is a necessary step for an effective environmental management of the natural resources of a river basin, as Lelis et al. (2012) points out.

In Brazil, the great thickness of the sedimentary rocks the Paraná River Basin accumulated over geological time favored water recharge, containing almost half of the groundwater reserves of the entire country. The alluvial plain of the Mogi Guaçu River is located in what is considered to be the largest national hydrogeological province and the dynamics of its groundwater vary seasonally, depending on the plain's degree of evolution and its fluvial conditions.

The understanding of the deposition processes and conformation of the relief, resulting from the soil-climate-flow interaction, is fundamental in the study of water dynamics and its interaction with the landscape. As the action of water wearing away the land surface, the soil becomes a testament to the evolutionary processes that shape the landscape (Mello et al., 2019). Thus, the hydrological processes associated with the generation of aquifer flow and recharge require complementary information regarding soil susceptibility to the detachment, transport and deposition processes that make up the water erosion, as well as its relationship with the landscape.

Research carried out in the region emphasizes the evolution of the silting potential and the consequent reduction in flow due to easy soil detachment combined with the low sediment transportation capacity of the drainage system (CPRM and CPLA, 2002; Klinke Neto et al., 2018). This process entails a strong tendency to dry up some watercourses in the short term (CPRM and CPLA, 2002) and highlights the urgency behind protecting the soil from the impact of raindrops and runoff. In addition to the local environmental characteristics, the erosive and depositional processes currently observed in the region are being accelerated due

to human action (dikes and/or dams, degraded areas, roads, among others) (Klinke Neto et al., 2018). Thus, studies that address the interaction between factors that act on soil erosion in the area are essential for actions aimed at soil and water conservation to be taken.

Vegetal cover, climate, soil class, and topography influence the erosive process, so the studies are based on the intense experimentation of these factors on the sediment production. In this sense, mathematical models are used to simulate the integration of the variables involved in the erosion and to evaluate the hydrological processes occurring in the environment. However, it should be emphasized, that an efficient evaluation requires erosion models that encompass certain variables in the topography analysis (Kandel et al., 2004), such as the contribution area (Moore and Burch, 1986; Desmet and Govers, 1996; Mitsova et al., 1996) and the points subjected to deposition in the hydrographic basin (Kinnell, 2005; Warren et al., 2005; Oliveira et al., 2013). Among these models, the Unit Stream Power Erosion and Deposition (USPED) (Mitsova et al., 1996) stands out.

Derived from the empirical hydrological model USLE (Universal Soil Loss Equation) (Wischmeier and Smith, 1978), the semi-empirical model USPED adds a physical base that attempts to compare the relief morphology to erosion-defining runoff parameters, making the estimation more accurate. The improvement of this model when compared to the USLE stimulated its study in several regions of the world, Africa (Tamene and Vlek, 2008), Europe (Niculiță, 2011; Rodriguez and Suarez, 2012; Sir et al., 2013; Aiello et al., 2015; Lazzari et al., 2015; Djodjic and Markensten, 2019; Honek et al., 2020), Asia (Kandrika and Dwivedi, 2003; Seo et al., 2010), North (Warren et al., 2005; Pricope, 2009; Warren et al., 2019) and South America (Oliveira et al., 2013). The USPED model's distinctive feature is that it predicts not only the spatial distribution of erosion but also deposition rates under laminar flow conditions and furrows in convergent and divergent terrain in large areas and high precipitation. The USPED model considers the flow strength unit theory to derive the topographic factor, which consists of a matching contribution area variable.

In this context, the current work aims to analyze erosion and deposition in a sub-basin on the Mogi Guaçu River's margins, municipality of Mogi Guaçu, SP, Brazil, using the USPED model. In addition to evaluating the associated factors and identifying the sources and sediment receiving areas, this study intends to generate subsidies for future diagnoses of areas with greater capacity for water storage in the Mogi Guaçu River plain. The loss of mineral and organic particles arising from the erosive process changes the soil's effective depth, texture and structure, directly and negatively impacting its capacity to absorb and retain water.

**MATERIALS AND METHODS**

**Study area**

The studied sub-basin has a surface area of 7.727 km<sup>2</sup> and is located on the northern margin of the upper middle course of the Mogi Guaçu River, in part of its alluvial

plain, in the municipality of Mogi Guaçu (SP) (Figure 1). The sub-basin is part of the Mogi Guaçu Conservation Units Complex (CUCMG), located in the transitional zone between the Savanna (Brazilian Cerrado) and Atlantic Forest biomes. Featuring the biotic characteristics of both biomes, it can be considered an ecotone while also including an important part of the Permanent

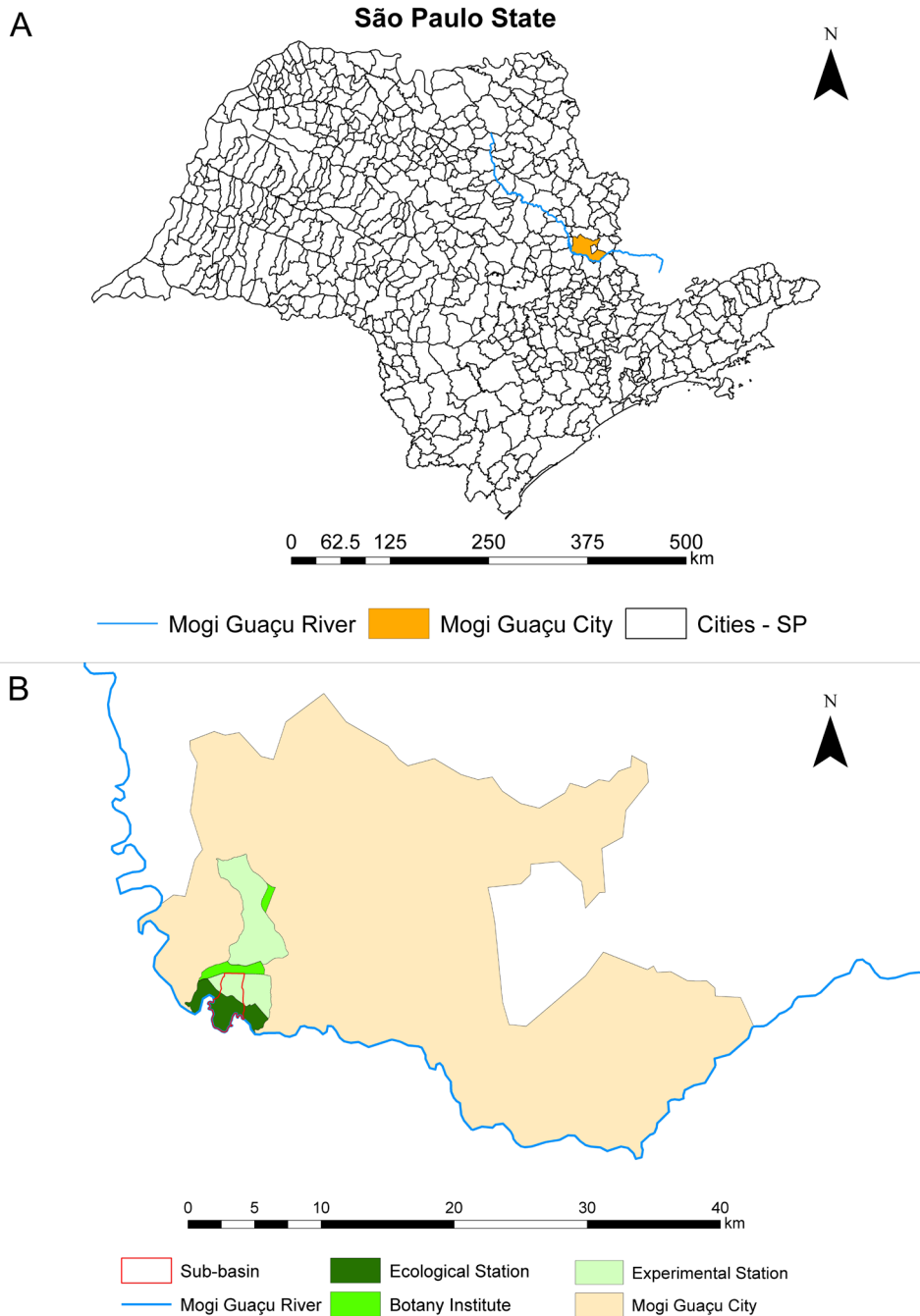


**Figure 1.** Location maps of the study sub-basin. (A) Regional, (B) Local.

Preservation Area (APP) of the Mogi Guaçu River, its sub-basins and springs.

The climate, according to the Koppen classification ranges between Aw (tropical climate with a dry winter season and rainy summer) and CWA (wet temperate climate with a dry winter and a hot summer) yearly average temperature of 21.5 °C and precipitation of 1,500 mm. In its geological context, the study area is regionally inserted in the Paraná Basin, characterized by the accumulation of a great thickness of sedimentary rocks. Locally, the study area is formed by sediments of the Itararé Subgroup, whose lithology is composed of fine sandstones, coarse conglomerates, clay, and clayey sandstone. The groundwater that occurs in the sedimentary rocks of this area is generally free, although it can occasionally be found at certain levels of confinement. Spatially well-defined reservoir layers are absent due to the great geological heterogeneity (Chang et al., 2003).

The soil map of the area has a scale of 1:30,000 (Figure 2A). Coming from the refinement of the semi-detailed survey (scale 1:100,000) (Oliveira et al., 1982), this map was produced during the preparation of the Management Plan for the Mogi Guaçu Conservation Units (UCRBEEc, 2010) and provided by the São Paulo State Forestry Institute (IF). The soils are classified according to the Brazilian Soil Classification System (SiBCS) (Embrapa Solos, 2018) and the current classes are Gleissolo Háplico Distrófico (GX), Gleissolo Melânico Distrófico (GM) (2.846 km<sup>2</sup>) and Latossolo Vermelho-Amarelo (LVA), with the LVA Distrófico cambissólico occupying 2.031 km<sup>2</sup> and the LVA Distrófico típico has 2.85 km<sup>2</sup>. LVA Distrófico cambissólico are soils with changeable primary materials visible in the profile and/or rock fragments on the B horizon at estimated percentages below incipient B horizon's limits within 200 cm of the soil surface (Embrapa Solos, 2018). Thus, the “cambissolic” distinction is presented as they present intermediate properties for the Cambissolos class. Furthermore, the place of occurrence of the LVA Distrófico cambissólico corresponds to terraces and the LVA Distrófico típico is located in floodplain areas with smooth undulating relief.

The soil textures in the study sub-basin are: LVA Distrófico cambissólico with loamy sand texture (15% clay, 10% silt, 75% sand); LVA Distrófico típico with sand clay loam texture (27% clay, 5% silt, 68% sand); and Gleissolo with loamy sand texture (15% clay, 8% silt, 77% sand). The sandy to medium texture of the study sub-basin soils is derived from the parent material of the Itararé Group sandstone. The texture data used for analysis in this article were obtained using a systematic survey (800 × 800 meters) conducted across sub-basin for mapping the soil properties, according to Klinke Neto et al. (2017). At each point, soil samples were collected according to Santos et al. (2005), in the 0 to 20 cm layer, representative of the surface diagnostic horizon. Particle size analysis was performed using the Bouyoucos method (Bouyoucos,

1951). The sand fraction was obtained by sieving. The North American Classification System (USDA) was used for the textural classification (Santos et al., 2005).

The relief information used in the analyzes comes from a Digital Elevation Model (MDE) built with a resolution of 10 meters, as a result of a planialtimetric survey (1:10,000 scale) conducted throughout the sub-basin (Figure 2B). The survey's goal was to study and learn about the preferential flows' directions paths and its influencers, as well as to improve the understanding of the relief relation versus the scale of analysis in landscape studies. The equipment used in the survey was the Topcon Hiper L1/L2 Geodetic Receiver, with a horizontal accuracy of 3 mm + 0.5 PPM and vertical accuracy of 5 mm + 0.5 PPM, with more than 5,000 points being collected for the relief description locally.

The mapping of land use was conducted with the ArcGIS 10.2 (ESRI, 2014) software and the information regarding the ground cover were obtained by interpreting CBERS-4 satellite image 10/01/2016, available for free at the Division Generation of Images (DGI) website created by the National Institute of Space Research (INPE, 2018). This information was complemented with field observations. The images were pre-treated (equalization), a composition of the bands of interest was made and then the map-to-map images were registered using the GeoCover image provided by National Aeronautics and Space Administration (NASA). The main classes mapped were: Submontane Semideciduous Seasonal Forest (FESD), Alluvial Semideciduous Seasonal Forest (FESDA) and vegetation with river influence (floodplains), according to the Technical Manual of Brazilian Vegetation (IBGE, 2012) (Figure 2C). Pinus and Eucalyptus forests, grassland not managed for about 20 years, and recovery areas with native species were also classified (Figure 2C). The floodplain areas are covered by dense shrubby vegetation with the sparse presence of lianas and herbaceous species. The coverage designated as recovering areas includes sites for the planting of native species in order to recover local vegetation.

## USPED modeling

The USPED model expresses soil loss by multiplying indexes that consider the effect of the following factors: rain (erosivity, R), soil (erodibility, K), topography (LS), cover and soil management (C) and conservationist practices (P). The work was carried out in a Geographic Information System (GIS) environment using the map algebra tool. Each of the K, LS, and C factors represent a specific map of the study area, generated with the spatial resolution of 10 m.

In addition to deposition, USPED results determine the surface affected by laminar erosion and rill erosion for each soil mapping unit. For the interpretation of soil losses estimated by the model, the criterion of soil losses tolerance was

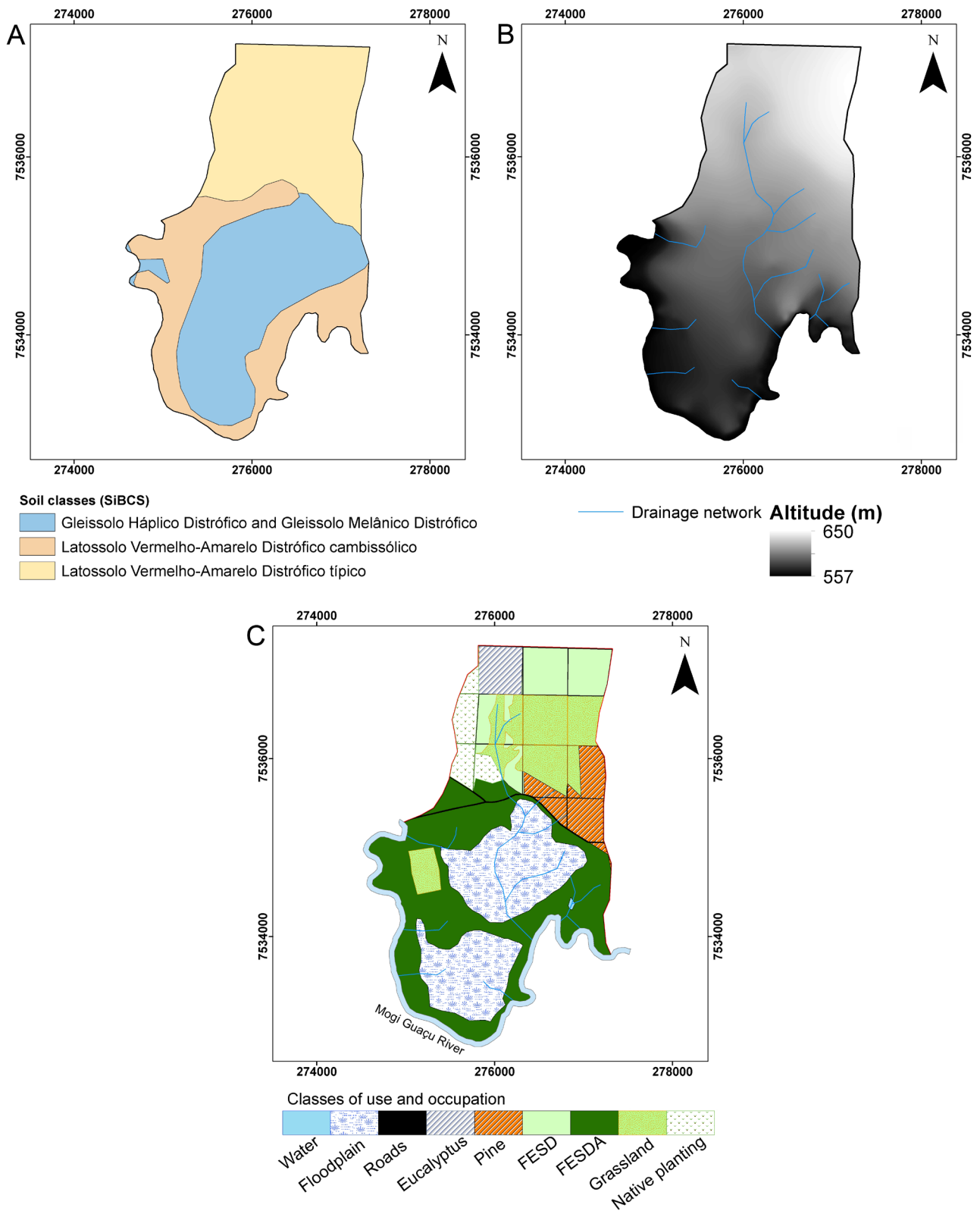


**Figure 2.** Sub-basin maps: (A) Soil classes; (B) Digital Elevation Model (MDE); (C) Classes of use and occupation. System of Coordinates UTM, datum SIRGAS 2000, zone 23S.

adopted as defined by Wischmeier and Smith (1978). Thus, the results were compared with the respective loss tolerances of  $11.53 \text{ t h}^{-1} \text{ year}^{-1}$  for the class Latossolo Vermelho-Amarelo and  $5.82 \text{ t ha}^{-1} \text{ year}^{-1}$  for the Gleissolo class. These values were estimated by Mannigel et al. (2002) for the State of São Paulo and correspond to the maximum loss that the soil supports to be able to recover through natural processes.

30 years of data (1970 to 1999) from the Brazilian National Water Agency (ANA) were used in the calculation of the annual R factor. The annual erosivity index (EI) was obtained by summing the monthly erosivity index calculated from Equation 1 (Lombardi Neto and Moldenhauer, 1992). The erosivity was then classified according to Foster et al. (1981).

$$\text{EI (R factor)} = 68.730 (p^2/P)^{0.841} \quad (1)$$

where:

EI = monthly average erosion index ( $\text{MJ mm ha}^{-1} \text{ h}^{-1} \text{ year}^{-1}$ );  
 p = mean monthly precipitation (mm);  
 P = mean annual rainfall (mm).

The K factor value was determined using the Bouyoucos model (Bouyoucos, 1935), which considers texture information in the analysis (Equation 2). In order to obtain the spatialisation of the variable, the equation was applied in each cell of the MDE (pixel-a-pixel), derived from the planialtimetric survey carried out in the area. The results of erodibility obtained were classified according to Foster et al. (1981).

$$\text{Factor K} = [(\text{sand (\%)} + \text{silt (\%)})] / (\text{clay (\%)})]/100 \quad (2)$$

where:

K Factor = soil erodibility ( $\text{Mg ha h ha}^{-1} \text{ MJ}^{-1} \text{ mm}^{-1}$ ).

The direction, distribution and consequent accumulation of the flow in an MDE are the main points to be controlled in a hydrological study. In the USPED model, the LS factor is given by Equation 3:

$$\text{LS} = A^m (\sin\theta)^n \quad (3)$$

where:

A = contribution area ( $\text{m}^2$ );  
 $\theta$  = slope angle;  
 m and n = constants that depend on the type of flow and soil properties.

For situations where rill erosion is dominant, these parameters are usually set at  $m = 1.6$  and  $n = 1.3$ ; and where laminar erosion prevails,  $m = n = 1.0$  (Foster and McCool, 1994). The parameters m and n were established as 1, due to the erosive laminar character found in the study sub-basin.

The contribution area was obtained from the MDE (Figure 2B), the slope maps (Figure 3A) and aspect maps were initially calculated, subsequently constructing the water flow paths.

The upstream contribution area map was determined from the lines of the water flow path and the DEM with 10 m spatial resolution (Figure 3B). The flow of each cell was obtained via the  $D_{\infty}$  method (Tarboton, 1997), as it better describes the surface flow pathways (Oliveira et al., 2012) and was similar to the drainage network observed in the field.

C factor ranges from 0 to 1 according to erosivity and erodibility, approaching zero in conservation management systems and 1 in non-conservation systems. The calculation of the C factor involves the data generated in the standard plots and the rain erosivity values to establish the soil loss ratio at each stage of the vegetation. Considering the amount of time spent and the cost of the direct evaluation of this factor in the field, in addition to the accuracy of the currently available methods that consider vegetation reflectance, C factor values were defined from the Normalized Difference Vegetation Index (NDVI) (Figure 3C). For the analysis of the vegetation through the NDVI, the CBERS-4 sensor image was composed of the visible band (R: band 3, G: band 2, B: band 1) and NDVI was processed with bands 3 (reflectance in red) and 4 (near infrared reflectance) (Asrar et al., 1984). This index is able to minimize topographic effects by producing a linear scale of measurement, which ranges from -1 (absence of vegetation) to +1 (high density of vegetation cover). Although they do not share the same proportionality, the scale of the C factor is inverse to that of the NDVI. Since the NDVI did not present negative values in this study, the values of C factor were defined from the inversion of the linear scale derived from the NDVI. The roads were mapped in the classification of use and occupation and transposed to the multispectral image, considering the low visualization of roads in the multispectral image for the analysis of NDVI and its importance in the soil losses of a basin with forest use.

The P factor ranges from 0 to 1, being equal to 1 when conservation practices are absent. The values for the P factor (dimensionless) were extracted from the literature. In the areas with natural vegetation (planted and native forests), the value of P was considered to be 0,10 (Roose, 1977), 0 (zero) in floodplain areas and water bodies and 1 for roads (Bertoni and Lombardi Neto, 2005).

In order to validate the spatialization accuracy of the erosion or depositional areas generated by the USPED model, 10 points classified as erosional areas, 10 points classified as depositional areas and 10 points classified as stable areas were selected on the map. The criteria behind selecting points was to check all kind of areas representing the diversity in environments and situations found in the field. The samples' purpose was to test the result generated when confronting contrast situations of classified

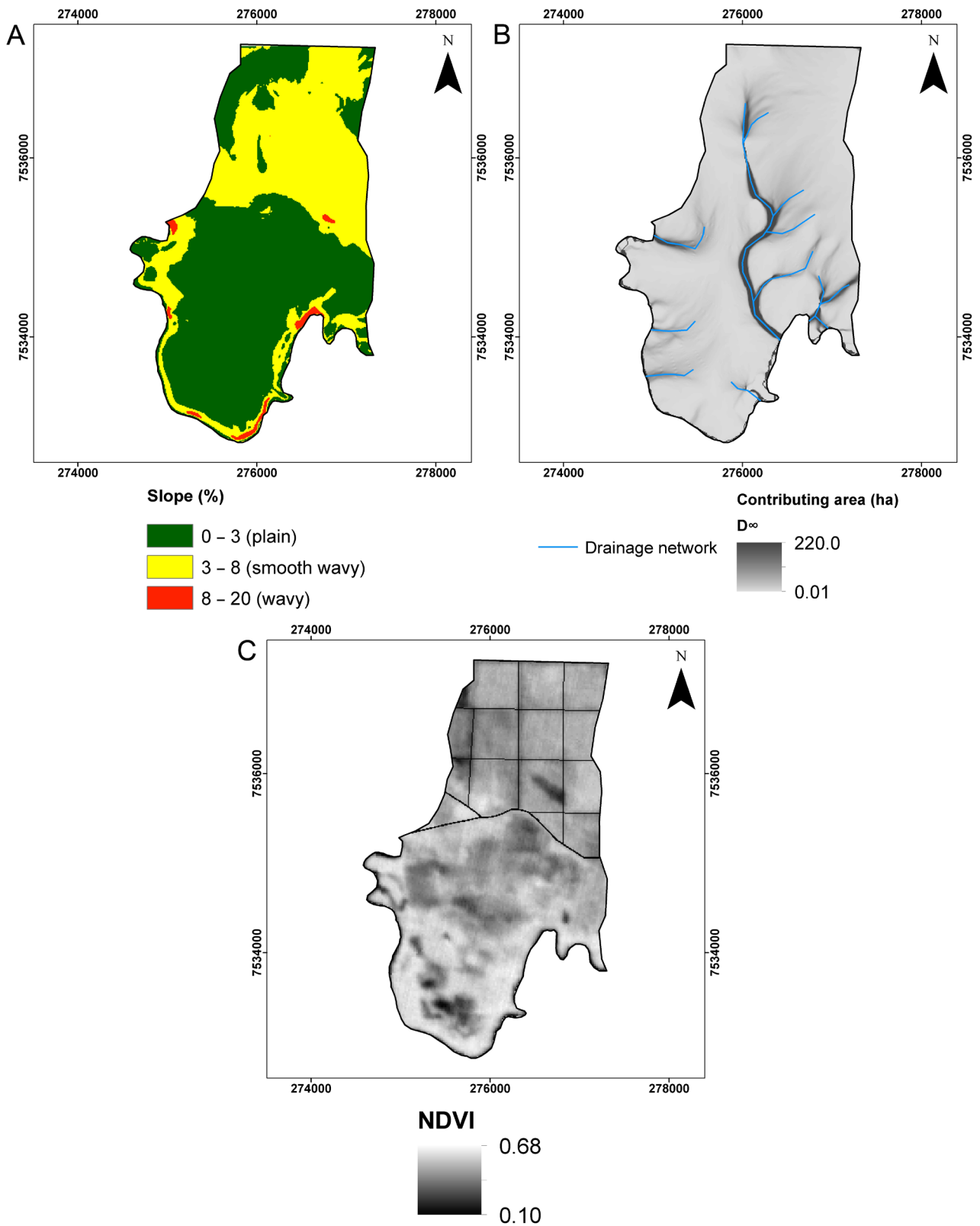


**Figure 3.** Variables generated for the modeling of the sub-basin: (A) Classes of the slope; (B) Contribution area; (C) Normalized Difference Vegetation Index (NDVI). System of Coordinates UTM, datum SIRGAS 2000, zone 23S.

areas as much as possible (abrupt change from one area to another), area gradient (gradual change between areas), homogeneous classification areas and fragmented areas. These points were used to confront the “ground truth”. Each point had its coordinates inserted into a Garmin 76 Csx GPS, which served as a guideline for the location of these points in the sub-basin. In the field, each selected point was surveyed and characterized as an eroded, deposited or stable area, based on the methodology adapted from Santos et al. (2005). The removal of surface and subsurface soil parts by the water action was detected by comparing the thickness of its surface horizon with another of the same type located in the area, in the same slope class, but in a portion where the erosive process did not occur. Deposition was considered when the soil surface presented loose and homogeneous particles distinct from the superficial horizon located below, without the presence of vegetation and, when pertinent, an overlay of the current vegetation was present. When the soil did not show erosion or apparent deposition signs, the area was classified as stable. The “ground truth” information was inserted and analyzed within the Kappa index with 95% confidence (Equation 4), where the hypotheses:  $H_0$  = null agreement and  $H_1$  = there is agreement.

$$\text{Kappa Index} = [P_o - P_c] / [1 - P_c] \quad (4)$$

where:

$P_o$  = proportion of units that fully agree;

$P_c$  = proportion of units that agree by chance.

## RESULTS AND DISCUSSION

### R, K, LS and C factors

The rainfall monthly average ranged from 32 to 253 mm, while the average annual rainfall was 1,460 mm. The values of monthly rainfall erosivity ranged from 52 to 1,652  $\text{MJ mm ha}^{-1} \text{h}^{-1}$ , with an annual average erosivity of 7,001  $\text{MJ mm ha}^{-1} \text{h}^{-1} \text{year}^{-1}$ . These values are considered critical, especially in the months of December, January and February. The annual average erosivity is classified as high and it is close to that verified by Weill et al. (2001) of 7.738  $\text{MJ mm ha}^{-1} \text{h}^{-1} \text{year}^{-1}$  for the Mogi Guaçu River basin, corresponding to the values expected for the region, according to Santa'anna Neto (1995).

Soil texture is an important factor that influences erodibility since it affects both the detachment process and the transport process associated with the erosion process. The soil erodibility (K factor) of the sub-basin ranged from 0.015 to 0.085  $\text{Mg ha h ha}^{-1} \text{MJ}^{-1} \text{mm}^{-1}$  (Figure 4A), being classified as low and high, respectively.

The lowest values of erodibility were observed in the areas presenting the Latossolo Vermelho-Amarelo Distrófico típico and correspond to the average value for this soil class in the State of São Paulo, as reported by Silva and Alvares (2005). The erodibility results estimated in this study correspond to those expected for Latossolos, whose low values are attributed to the variable amounts of iron and aluminum oxides which, by favoring aggregation and providing greater resistance to dispersion in water, are responsible for its good structure. Oxidized soils, even when very clayey, present low erodibility due to their good infiltration capacity. The highest values, verified in the Gleissolo area, are higher than the average observed in the State but are within the range expected for the class (Silva and Alvares, 2005). The areas of the basin with greater sand content, south and southeast, and higher silt, south and along the north bank of the Mogi Guaçu presented greater erodibility values (Figure 4A) while areas of low erodibility were associated with higher clay and lower sand contents, such as the north and northwest areas. It can also be added that fine particles (clay) tend to resist peeling, while larger particles (very coarse, coarse sand and medium sand) tend to resist transport. The silt and fine sand sizes are the most susceptible to both detachment and transport.

In the USPED model, the LS factor represents an interaction between the change in transport capacity (slope) and flow direction (aspect). The contribution area is, by definition, the representation of the water flow at a given site or grid of cells and is considered in the calculation of the LS factor of the model along with the aspect and slope maps of the area. The LS factor found was mainly low in a large part of the basin, being highest only in the slope and gully areas of the Mogi Guaçu River and in the higher elevated areas with the hill slope present in the upper middle part of the sub-basin, to the beginning of the main drain line (Figure 4B).

The C factor derived from NDVI (pixel-a-pixel) enabled a more accurate coverage analysis, rather than the establishment of a single C factor per coverage class. C factor values ranged from 0.10 to 0.68 (Figure 4C) and it was found that the variations in coverage density in the different plant classes present in the sub-basin were adequately represented by NDVI, as that's also observed in the studies by Carvalho et al. (2014), when estimating the C factor using NDVI for the RUSLE model, and Silva et al. (2013) and Silva et al. (2017) for the USLE model. In the analysis of the C factor derived from the intensity of the photosynthetic activities by the NDVI, it was possible to point out that the vegetation with the highest quantity of biomass, identified by the darker shades of gray (lower values), are more frequent in the southern part of the sub-basin that is mainly occupied by the native FESDA vegetation along the Mogi Guaçu River's margins (Figure 2C). The northern part of

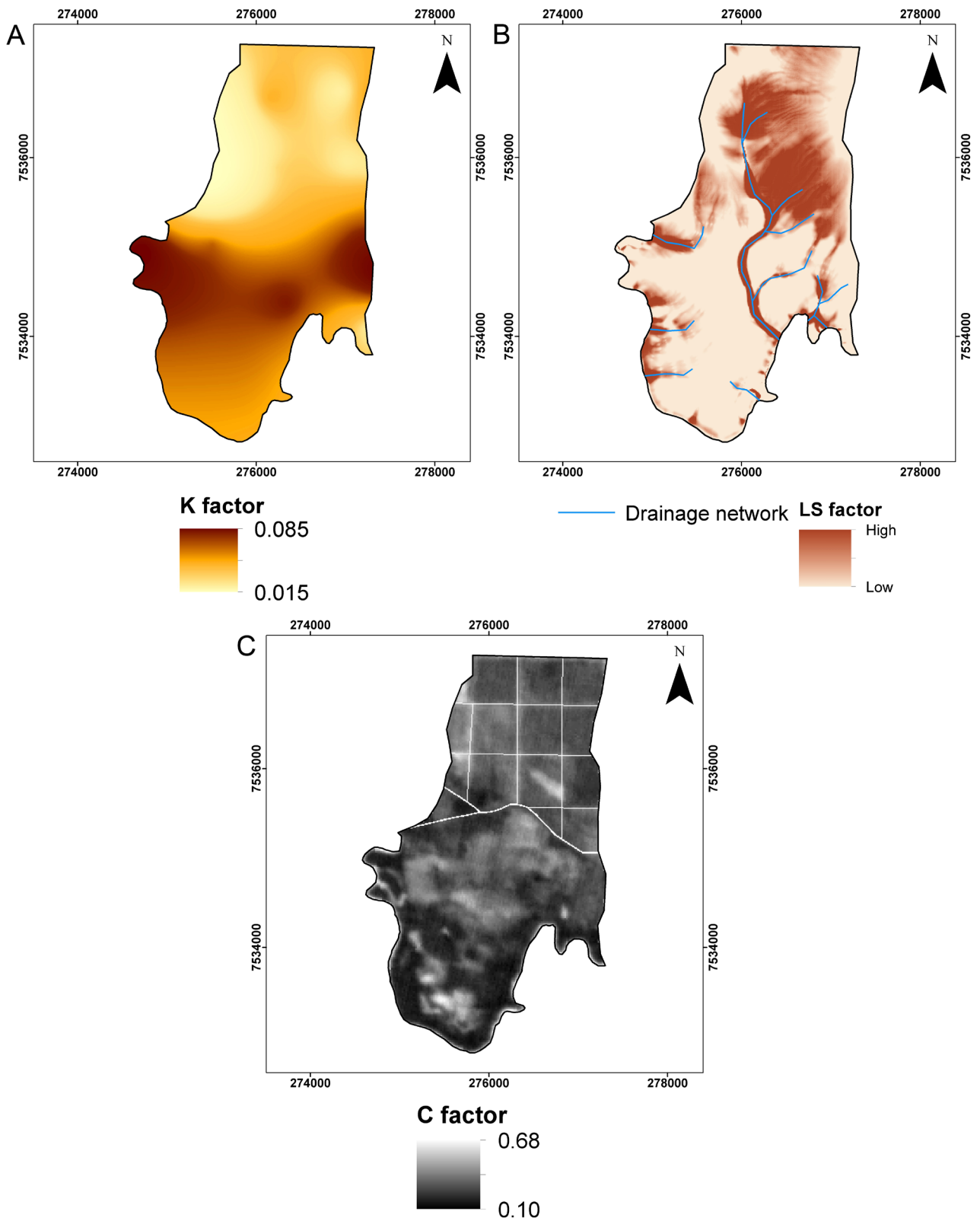


**Figure 4.** Factors of the USPED model: (A) K factor — Erodibility; (B) LS factor — Topography; (C) C factor — Land use and coverage. System of Coordinates UTM, datum SIRGAS 2000, zone 23S.

the area, represented by medium to low-density vegetation (lighter shades of gray) corresponds mainly to grasslands and planted forests. The higher values of the C factor mark the regions of exposed soil regarding the areas undergoing recovery or the degraded grasslands. Therefore, these regions are more prone to water erosion. There are still areas without vegetation related to roads, which naturally have high C factor values.

### USPED modeling

The USPED model provides estimates of annual average soil loss rates as well as the spatialization of erosion and deposition at basin scale from R, K, LS, C and P factors. The results found via modeling were classified as according to the following classes shown in Table 1: High Erosion; Moderate erosion; Low erosion; Very low erosion; Stable (erosion and deposition practically absent); Very low deposition; Low Deposition; Moderate deposition; High Deposition.

The result of the USPED model coupled with the erosion/deposition spatial distribution in the sub-basin as well as the points used in the validation process is presented in Figure 5. Stable areas, that is, that do not present erosion or deposition, represented approximately 60% of the sub-basin, according to the low-lying relief found in the area. Thus, surface runoff tends to be naturally slow to very slow in most soils and the infiltration process is facilitated, resulting in the stability of much of the basin. The erosion areas totaled 23.42% and, to a large extent (19.21%) were classified as very low erosions. Less than 1% of the total area presented losses above the tolerated limit (Table 1).

When the erosion process is observed in comparison to the soil classes, it is verified that the Latossolos presented a greater area subjected to erosion or deposition, with about 26 and 17% of their total area, when compared to the Gleissolos, which presented about 19 and 14%, respectively. Despite the smaller absolute area affected by erosion in the Gleissolos, this class presented proportionally, more than twice the areas above the tolerated limit in comparison to the Latossolos (Table 1). When comparing the highest values of erodibility verified for the Gleissolos and the lowest values, when compared to the Latossolos, it is verified that other factors of the USPED model are interfering in the erosive dynamics of the sub-basin. Since rainfall erosivity is the same throughout the area, due to its small size, we can see the marked influence of the topography and the vegetation cover in the modeling process. Grasslands mainly characterize the less dense vegetation that increases the susceptibility to erosion in the sub-basin and pine forests, as presented in the C factor (Figure 4C).

At the sites of intermediate LS factor (Figure 4B) the erosion will occur at a low intensity, whereas very low ones correspond to parts of undulated relief (3 to 8% slope) of

the sub-basin (Figure 3A). The most susceptible areas to the erosive process (high and moderate erosion) are subjected to the drainage network flow convergence and/or located in regions of greater slope (8 to 20%, undulated relief) near the Mogi Guaçu River, represented by the high values of the LS factor. In the areas to the northeast of the sub-basin, the relief is undulating, and the soil cover is less protective (Figure 4C), favoring erosion. In the southern part of the sub-basin, where the low LS factor (Figure 4B) reflects the predominantly flat relief (0 to 3% slope), there is a greater influence of soil class and vegetation cover, corroborating the verification of Aiello et al. (2015) regarding the greater relevance of these factors over the others when analyzing the USPED in conditions of smooth topography. In this sense, the application of the USPED model in rugged topography by Sir et al. (2013), showed higher erosion rates derived from the combination of the topography associated with susceptible soils and intensive agriculture.

On the Mogi Guaçu River's margins, geomorphologically related to alluvial terraces and unconsolidated sediments, the largest erosion is related to the undulating soft relief associated with the Latossolo Vermelho-Amarelo Distrófico cambissólico adjacent to the river, which is high erodibility soil in the region due to cambisolic property (Figure 5). As for the Gleissolos of the sub-basin, although they present high erodibility (Figure 4A), they are found in alluvial deposits that undergo periodic flooding and are located in flat areas that cover about 60% of the entire basin (463.62 ha) (Figure 3A) and are thus less susceptible to erosion, representing the stable areas (Table 1 and Figure 5).

It is important to highlight the impact of roads in the area, which are one of the main causes of erosion and sediment sources in sub-basins (Figure 5). In this sense, the results estimated by USPED correspond to what was verified in the field. The roads are located in the greater slope of the basin (Figures 2C and 3A) which, combined with the high rainfall erosivity, contributes to the soil losses in these segments. The road network of the sub-basin presents an orthogonal constructional pattern, where the roads are constructed parallel to each other, at symmetrical distances and cut perpendicularly, not considering the characteristics of the relief and hydrography. The pattern of construction is simple, with no primary coating on the bearing surface and soil conservation work, making them more susceptible to climatic influences. In the rainy periods during the months of December, January and February, the erosive process is evidenced from the action of surface runoff since, with the central belt of the road waterproofed due to compaction, the road acts as a canal carrying water and sediments. The water accumulates along the roadsides and is directed towards the slope, which, in addition to concentrating great destructive force and soil drag, impairs recharge in the sub-basin as this water can no longer infiltrate, and favors siltation and water source

**Table 1.** Estimation of loss and soil deposition by the USPED model and tolerance of soil loss, in comparison to the total surface and sub-basin soil classes.

Classes (Mg ha <sup>-1</sup> year <sup>-1</sup> )	% total surface (100%)	% Latossolos (63%)	% Gleissolos (37%)
High erosion (> 50)	0.02	0.03	0
Moderate erosion (49 to 5)	1.22	1.13	1.39
Low erosion (4.9 to 1)	2.97	3.08	2.80
Very low erosion (0.99 to 0.1)	19.21	21.82	14.77
Stable (0.09 erosion to 0.1 deposition)	60.82	57.24	66.90
Very low deposition (0.11 to 1)	11.99	13.09	10.11
Low Deposition (1.1 to 5)	2.45	2.39	2.55
Moderate Deposition (5.1 to 50)	1.31	1.21	1.47
High Deposition (> 50.1)	0.01	0.02	0
Tolerance of soil losses	----- % -----		
<Tolerance	99.22	99.46	98.81
> Tolerance	0.78	0.54	1.19

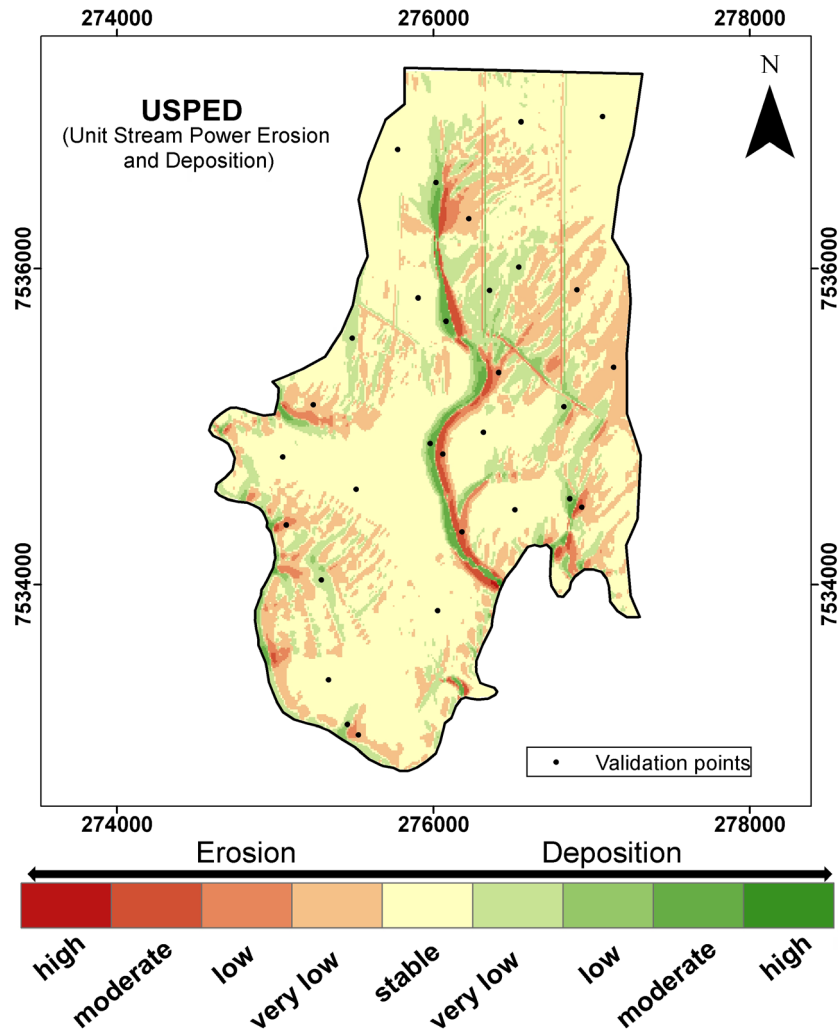


**Figure 5.** Erosion and deposition potential estimated using the USPED model, in the Mogi Guaçu River sub-basin. UTM System of Coordinates, SIRGAS 2000 datum, zone 23S.

pollution. Due to these reasons, roads require careful management and permanent conservation.

The depositional areas represented 15.76% of the sub-basin's total surface, classified in the very low class in the majority (Table 1). Throughout the sub-basin, there is a pattern of erosion and deposition sites. In general, these sites are adjacent to one another and occur preferably near or within the drainage network (Figure 5), also seen in the Tamene and Vlek (2008), Seo et al. (2010) and Aiello et al. (2015) studies during the application of the USPED model. Deposition points in the flat areas south of the basin were observed, corroborating the observations of Sir et al. (2013) regarding the deposition of sediments in the flat parts of the relief in a basin, and not only the bottoms of valleys and hillside slopes.

The vegetation cover exerts a noticeable influence on the susceptibility to erosion and deposition processes in the sub-basin. The FESD present in the areas of undulating soft relief (Figures 2C and 3A) is more protective when compared to planted forests (*Pinus* and *Eucalyptus*) and grasslands in areas of the same topography. By protecting the soil against erosion degradation, water that could be lost through runoff infiltrates the soil and percolates to deeper layers, supplying the aquifers. Thus, the native forest contributes in an effective way for the soil to maintain its function as a way of rainwater entering the hydrographic basin and, consequently, interfering with the local hydrological system. When evaluating soil loss in comparison to the use in the Mogi Guaçu River basin, Weill et al. (2001) also reported greater erosion in the grassland rather than in the native forest.

In the FESDA vegetation areas located on the Mogi Guaçu River's margins, erosion was observed associated with the rugged topography and the deposition was favored by litter and native forest vegetation. Plant residues in direct contact with the soil surface reduce the sediment load in the runoff since they act as a network by filtering sediments suspended in the runoff. Thus, the riparian forest interferes in the dynamics of surface water in detriment of groundwater and in the depositional processes that form the physical environment that sustains it. These results are concordant with the one pointed out by Lima et al. (2005), which affirms that the soil cover is a very active factor in the definition of the recharge potential, as well as erosive and depositional behavior of eroded slope sediments, as well as soil type, topography, and rainfall, since the vegetation cover affects soil attributes, distribution and abundance of water in the soil.

The results obtained by the Kappa Index (Table 2) revealed that the USPED model obtained an excellent agreement with the "ground truth" regarding the spatialisation question, reaching the general value of 0.85, which according to Landis and Koch (1977) is interpreted as a very high match between the field data and the model. Only in the stable areas, the correlation was below the optimum limit of 0.85, yet it is still considered to be good.

The results estimated by USPED in the sub-basin are concordant to those reported by Weill et al. (2001), Boumanns et al. (2010) and IPT (2012), which highlight a medium to low susceptibility to erosion throughout the sub-basin. In a region close to the study area, inserted in the Mogi Guaçu River basin, Fushita et al. (2011) also estimated low to medium erosion risk. IPT (2012) reported a moderate to high sedimentation trend in the study area, including the Mogi Guaçu River, overestimating the results observed in the current study, where about 60% of the area is stable (with erosion ranging from 0 to 0.09 Mg ha<sup>-1</sup> year<sup>-1</sup>, and deposition of 0 to 0.1 Mg ha<sup>-1</sup> year<sup>-1</sup>) and 11.99% presented very low deposition (< 1 Mg ha<sup>-1</sup> year<sup>-1</sup>) (Table 1). In the surveys carried out by Weill et al. (2001) and Boumanns et al. (2010) using the USLE model, soil losses in the sub-basin region occurred predominantly in the range of 14 to 28 Mg ha<sup>-1</sup> year<sup>-1</sup> and 0 to 24 Mg ha<sup>-1</sup> year<sup>-1</sup>, respectively. This range indicates an overestimation of this model compared to the USPED model, which estimated about 20% of the area with losses of 0.1 to 0.99 Mg ha<sup>-1</sup> year<sup>-1</sup>, in addition to a large part of the sub-basin (60.82%) practically free of losses and deposition (Table 1). We consider the results of the current study to be more accurate since the USLE presents the limitation of considering an average slope (S factor) and slope length (L factor) for the entire basin, so that the direct influence of the convergent and divergent flow, that is, of the surface runoff, is minimized, making it impossible to determine the sources and sinks of the erosion materials and deposition areas. The water erosion, as a process directed hydrologically, must be assessed in terms of runoff and detail (pixel by pixel), which is performed by USPED (Kandel et al., 2004; Warren et al., 2005; Oliveira et al., 2013).

Several studies have demonstrated the ability of USPED to estimate realistic rates of soil loss and deposition compared to other models. Warren et al. (2019) found similar results such as those observed in this study using, from the visual analysis of the erosion and deposition points in field, the qualitative validation of the USPED model, achieving

**Table 2.** Kappa index result for validation of USPED model spatialization.

	Erosion	Deposition	Stable	General
Kappa Index	0.927	0.850	0.769	0.850
P	< 0.001	< 0.001	< 0.001	< 0.001
Confidence Interval (95%)	1 – 0.57	1 – 0.492	1 – 0.412	1 – 0.597

90% of hits with the USPED estimation. In addition to the potential of this validation type, the cited authors recommend the model highlighting its accuracy and simplicity to provide information regarding the erosion and deposition locations in addition to intensity and distribution, allowing for effective and punctual actions regarding the soil conservation.

Aiello et al. (2015) and Lazzari et al. (2015), when comparing the performance of the USPED model with dam siltation data collected in the field, verified that the model estimated values very close to those observed, confirming its reliability in the quantification of erosion at the basin scale. The authors attributed this performance to the presence of the contribution area as a USPED calculation variable since it reflects the impacts of the divergent and convergent flow. Warren et al. (2005) and Tamene and Vlek (2008) also reported a high level of agreement between the results estimated by USPED and those collected in the field.

## CONCLUSIONS

60% of the sub-basin's area was unaffected by considerable erosion and deposition, both due to the current arboreal vegetation, but also the flat or low-lying relief of the site. Thus, the runoff tends to be slow or very slow for most soils and the infiltration process is facilitated. The stability of the sub-basin in terms of erosion favors the recharge of water in the area since the soils present a sandy texture and the Latossolos, which comprise most of the sub-basin, are deep, thus possessing a high storage capacity of water and permeability.

In the rest of the area, erosion points totaled 23.42%, largely classified as very low erosion, and less than 1% of the total area presented losses above the tolerated limit. In these areas, the evolution of the erosive process is favored, mainly in greater slopes, by the sandy texture of the soil that results in the low aggregation of particles. The areas of moderate to high susceptibility to the erosive process are those subjected to the convergence of flow of the drainage network and occupied mainly by grasslands, Pinus forest, and roads. Under the same conditions, but with native forest vegetation (FESD), the soil is better protected and the water, which could be lost through the surface runoff, infiltrates and percolates to the deeper layers of the profile, supplying the aquifers. Therefore, the native forest collaborates so that the soil maintains its role as means of entry of rainwater into the river basin and, consequently, interferes with the local hydrological system.

There is a pattern of erosion and deposition sites, which are adjacent to one another and occur preferably near or within the drainage network. The deposition areas accounted for 15.76% of the sub-basin's total surface, being classified in the very low class for the most part. The deposition of the

material transported from the slopes in the drainage network increases the risk of affecting the water quality and availability of the water bodies due to the silting.

The validation of the spatialisation obtained by the USPED model revealed a very high correspondence between the field data and the model. The USPED allowed identifying the preferential paths of the surface runoff in the Mogi Guaçu River sub-basin, directly associated with the development of the erosive process. It was also possible to see how the hydrological cycle, the soils, and the vegetation interact with each other. Thus, it was possible to delimit the priority areas during conservation intervention, characterized by grasslands, Pinus forest and sub-basin roads, located mainly in stretches of rugged relief. Assessment, prevention and control of the erosion in the sub-basin are key issues in order to maintain and ensure adequate soil hydrological responses and reduce hydrogeological risk.

## ACKNOWLEDGMENTS

The authors would like to thank CAPES and CNPq for granting the scholarships; the São Paulo State Research Support Foundation (FAPESP) for financing the project (Nº 2013 / 22729-2); and the Forest Institute (IF-SP) for logistical support to conduct the study.

## REFERENCES

- Aiello, A., Adamo, M., Canora, F. (2015). Remote sensing and GIS to assess soil erosion with RUSLE3D and USPED at river basin scale in southern Italy. *Catena*, 131, 174-185. <https://doi.org/10.1016/j.catena.2015.04.003>
- Asrar, G., Fuchs, M., Kanemasu, E. T., Hatfield, J. L. (1984). Estimating absorbed photosynthetic radiation and leaf area index from spectral reflectance in wheat. *Agronomy Journal*, 76(2), 300-306. <https://doi.org/10.2134/agronj1984.00021962007600020029x>
- Bertoni, J., Lombardi Neto, F. (2005). *Conservação do solo*. São Paulo: Ícone.
- Boumanns, R., Ambrósio, L. A., Romeiro, A. R., Campos, E. M. G., Fasiaben, M. C. R., Andrade, D. C., Tôsto, S. G., Moraes, J. F. L., Camargo, L. A. S., Sinisgalli, P. A. A., Sousa Junior, W. C. (2010). Modelagem dinâmica do uso e cobertura das terras para o controle da erosão na bacia hidrográfica do Rio Mogi-Guaçu e Pardo, São Paulo - Brasil. *Revista Iberoamericana de Economía Ecológica*, 14, 1-12. Available at: <https://raco.cat/index.php/Revibec/article/view/200504>. Accessed on: Jan 17, 2022.

- Bouyoucos, G. J. (1935). The Clay ratio as a criterion of susceptibility of soils to erosion. *Journal of the American Society of Agronomy*, 27(9), 738-741. <https://doi.org/10.2134/agronj1935.00021962002700090007x>
- Bouyoucos, G. J. (1951). A recalibration of the hydrometer method for making mechanical analysis of soil. *Agronomy Journal*, 43(9), 434-438. <https://doi.org/10.2134/agronj1951.00021962004300090005x>
- Carvalho, D. F., Durigon, V. L., Antunes, M. A. H., Almeida, W. S., Oliveira, P. T. S. (2014). Predicting soil erosion using Rusle and NDVI time series from TM Landsat 5. *Pesquisa Agropecuária Brasileira*, 49(3), 15-224. <https://doi.org/10.1590/S0100-204X2014000300008>
- Cecílio, R. A., Martinez, M. A., Pruski, F. F., Silva, D. D. (2013). Modelo para estimativa da infiltração de água e perfil de umidade do solo. *Revista Brasileira de Ciência do Solo*, 37(2), 411-421. <https://doi.org/10.1590/S0100-06832013000200012>
- Chang, H. K., Teixeira, A. J., Vidal, A. C. (2003). Aspectos hidrogeológicos e hidroquímicos das regiões dos municípios de Mogi Mirim, Mogi Guaçu e Itapira no Estado de São Paulo. *Revista Geociências*, 22(Especial), 63-73. Available at: [https://www.revistageociencias.com.br/geociencias-arquivos/22\\_especial/6.PDF](https://www.revistageociencias.com.br/geociencias-arquivos/22_especial/6.PDF). Accessed on: Jan 17, 2022.
- Desmet, P. J. J., Govers, G. (1996). A GIS procedure for automatically calculating the USLE LS factor on topographically complex landscape units. *Journal of Soil and Water Conservation*, 51(5), 427-433. Available at: <https://www.jswconline.org/content/51/5/427>. Accessed on: Jan 17, 2022.
- Djordjic, F., Markensten, H. (2019). From single fields to river basins: Identification of critical source areas for erosion and phosphorus losses at high resolution. *Ambio*, 48, 1129-1142. <https://doi.org/10.1007/s13280-018-1134-8>
- Empresa Brasileira de Pesquisa Agropecuária (EMBRAPA Solos). (2018). *Sistema brasileiro de classificação de solos*. 5ª ed. Brasília: EMBRAPA Solos.
- Environmental Systems Research Institute (ESRI). (2014). *ArcGIS Professional GIS for the desktop*. Version 10.2. Redlands: ESRI.
- Foster, G. R., McCool, D. K. (1994). Comment on "Length-slope factors for the Revised Universal Soil Loss Equation: simplified method of estimation". *Journal of Soil and Water Conservation*, 49(2), 171-173. Available at: [link.gale.com/apps/doc/A15406377/AONE?u=anon~3b77cf71&sid=googleScholar&xid=fea18146](http://link.gale.com/apps/doc/A15406377/AONE?u=anon~3b77cf71&sid=googleScholar&xid=fea18146). Accessed on: Jan 17, 2022.
- Foster, G. R., McCool, D. K., Renard, K. G., Moldenhauer, W. C. (1981). Conversion of the universal soil loss equation to SI metric units. *Journal of Soil and Water Conservation*, 36(6), 355-359. Available at: <https://www.jswconline.org/content/36/6/355>. Accessed on: Jan 17, 2022.
- Fushita, A. T., Camargo-Bortolin, L. H. G., Arantes, E. M., Moreira, M. A. A., Cançado, C. J., Lorandi, R. (2011). Fragilidade ambiental associada ao risco potencial de erosão de uma área da região geoeconômica médio Mogi Guaçu superior (SP). *Revista Brasileira de Cartografia*, 63(4), 477-488. Available at: <https://seer.ufu.br/index.php/revistabrasileiracartografia/article/view/49216>. Accessed on: Jan 17, 2022.
- Honek, D., Michalková, M. S., Smetanová, A., Sočuvka, V., Velísková, Y., Karásek, P., Konečná, J., Némětová, Z., Danáčová, M. (2020). Estimating sedimentation rates in small reservoirs - Suitable approaches for local municipalities in central Europe. *Journal of Environmental Management*, 261, 109958. <https://doi.org/10.1016/j.jenvman.2019.109958>
- Instituto Brasileiro de Geografia e Estatística (IBGE). (2012). *Manual técnico da vegetação brasileira*. Rio de Janeiro: IBGE.
- Instituto de Pesquisas Tecnológicas (IPT). (2012). *Relatório técnico nº 131.057-205 do IPT sobre o cadastramento de pontos de erosão e inundação no Estado de São Paulo*. São Paulo: IPT. Available at: [https://sigrh.sp.gov.br/public/uploads/documents/7421/erosoes\\_dossie-das-ugrhis.pdf](https://sigrh.sp.gov.br/public/uploads/documents/7421/erosoes_dossie-das-ugrhis.pdf). Accessed on: Jan 17, 2022.
- Instituto Nacional de Pesquisas Espaciais (INPE). (2018). *Catálogo de imagens*. Available at: <http://www.dgi.inpe.br/CDSR>. Accessed on: Jan 10, 2018.
- Kandel, D. D., Western, A. W., Grayson, R. B., Turrall, H. N. (2004). Process parameterization and temporal scaling in surface runoff and erosion modelling. *Hydrological Processes*, 18(8), 1423-1446. <https://doi.org/10.1002/hyp.1421>
- Kandrika, S., Dwivedi, R. S. (2003). Assessment of the impact of mining on agricultural land using erosion-deposition model and space borne multispectral data. *Journal of Spatial Hydrology*, 3(2), 1-17. Available at: <https://scholarsarchive.byu.edu/josh/vol3/iss2/1>. Accessed on: Jan 17, 2022.

- Kinnell, P. I. A. (2005). Why the universal soil loss equation and the revised version of it do not predict event erosion well. *Hydrological Processes*, 19(3), 851-854. <https://doi.org/10.1002/hyp.5816>
- Klinke Neto, G., Oliveira, A. H., Pereira, S. Y. (2017). Variabilidade espacial de atributos físicos do 523 solo em planície aluvionar do Rio Mogi Guaçu (SP). *Geociências*, 36(2), 381-394. <https://doi.org/10.5016/geociencias.v36i2.12593>
- Klinke Neto, G., Oliveira, A. H., Pereira, S. Y. (2018). Fisiografia e geomorfologia em sub-bacia da planície do Rio Mogi Guaçu, Estado de São Paulo, Brasil. *Anuário do Instituto de Geociências*, 41(2), 177-190. [https://doi.org/10.11137/2018\\_2\\_177\\_190](https://doi.org/10.11137/2018_2_177_190)
- Landis, J. R., Koch, G. G. (1977). The measurement of observer agreement for categorical data. *Biometrics*, 33(1), 159-174. <https://doi.org/10.2307/2529310>
- Lazzari, M., Gioia, D., Piccarreta, M., Danese, M., Lanorte, A. (2015). Sediment yield and erosion rate estimation in the mountain catchments of the Camastra artificial reservoir (Southern Italy): a comparison between different empirical methods. *Catena*, 127, 323-339. <https://doi.org/10.1016/j.catena.2014.11.021>
- Lelis, T. A., Calijuri, M. L., Santiago, A. F., Lima, D. C., Rocha, E. O. (2012). Análise de sensibilidade e calibração do modelo SWAT aplicado em bacia hidrográfica da região sudeste do Brasil. *Revista Brasileira de Ciência do Solo*, 36(2), 623-634. <https://doi.org/10.1590/S0100-06832012000200031>
- Lima, J. E. F. W., Lopes, W. T. A., Carvalho, N. O., Vieira, M. R., Silva, E. M. (2005). Suspended sediment fluxes in the large river basins of Brazil. *Seventh IAHS Scientific Assembly*, 1, 355-363. Available at: <https://iahs.info/uploads/dms/13042.48%20355-363%20S11-19%20Werneck%20et%20al.pdf>. Accessed on: Jan 17, 2022.
- Lombardi Neto, F., Moldenhauer, W. C. (1992). Erosividade da chuva: sua distribuição e relação com as perdas de solo em Campinas (SP). *Bragantia*, 51(2), 189-196. <https://doi.org/10.1590/S0006-87051992000200009>
- Mannigel, A. R., Carvalho, M. P., Moreti, D., Medeiros, L. R. (2002). Fator erodibilidade e tolerância de perda dos solos do Estado de São Paulo. *Acta Scientiarum*, 24(5), 1335-1340. <https://doi.org/10.4025/actasciagron.v24i0.2374>
- Mello, C. R., Norton, L. D., Pinto, L. C., Curi, N. (2019). *Hydropedology in the tropics*. Lavras: UFLA.
- Mitasova, H., Hofierka, J., Zlocha, M., Iverson, L. R. (1996). Modelling topographic potential for erosion and deposition using GIS. *International Journal Geographical Information System*, 10(5), 629-641. <https://doi.org/10.1080/02693799608902101>
- Moore, I. D., Burch, G. J. (1986). Physical basis of the length-slope factor in Universal Soil Loss Equation. *Soil Science Society of America Journal*, 50(5), 1294-1298. <https://doi.org/10.2136/sssaj1986.03615995005000050042x>
- Nearing, M. A., Wei, H., Stone, J. J., Pierson, F. B., Spaeth, K. E., Weltz, M. A., Flanagan, D. C., Hernandez, M. (2011). A rangeland hydrology and erosion model. *Transactions - American Society of Agricultural Engineers*, 54(3), 901-908. <https://doi.org/10.13031/2013.37115>
- Niculită, I. C. (2011). Sheet and rill soil erosion estimation for agricultural land evaluation. *Bulletin UASVM Agriculture*, 68(1), 237-244. <https://doi.org/10.15835/buasvmcn-agr:6447>
- Oliveira, A. H., Silva, M. A., Silva, M. L. N., Curi, N., Klinke Neto, G., Freitas, D. A. F. (2013). Development of topographic factor modeling for application in soil erosion models. In: M. C. H. Soriano (Ed.). *Soil processes and current trends in quality assessment*, 1, 111-138. Croatia: InTeh. <https://doi.org/10.5772/54439>
- Oliveira, A. H., Silva, M. L. N., Curi, N., Klinke Neto, G., Silva, M. A., Araújo, E. F. (2012). Consistência hidrológica de modelos digitais de elevação (MDE) para definição da rede de drenagem na sub-bacia do horto florestal Terra Dura, Eldorado do Sul, RS. *Revista Brasileira de Ciência do Solo*, 36(4), 1259-1267. <https://doi.org/10.1590/S0100-06832012000400020>
- Oliveira, J. B., Barbieri, J. L., Rotta, C. L., Tremocoldi, W. (1982). *Levantamento pedológico semidetalhado do Estado de São Paulo: Quadricula de Araras*. Campinas: Instituto Agrônomo. Mapa, escala 1:100.000. (Boletim Técnico, 72.)
- Pricope, N. (2009). Assessment of spatial patterns of sediment transport and delivery for soil and water conservation programs. *Journal of Spatial Hydrology*, 9(1), 21-46. Available at: <https://scholarsarchive.byu.edu/josh/vol9/iss1/1>. Accessed on: Jan 17, 2022.
- Rodriguez, J. L. G., Suarez, M. C. G. (2012). Methodology for estimating the topographic factor LS of RUSLE3D and USPED using GIS. *Geomorphology*, 175-176, 98-106. <https://doi.org/10.1016/j.geomorph.2012.07.001>

- Roose, E. I. (1977). Application of the universal soil loss equation of Wischmeier and Smith in West Africa. In: D. J. Greenland, R. Lal (Eds.). *Soil conservation and management in the humid tropics*, 1, 177-187. Proceedings of the International Conference. Chichester: John Wiley and Sons.
- Santa'anna Neto, J. L. (1995). A erosividade das chuvas no Estado de São Paulo. *Revista do Departamento de Geografia*, 9, 35-49. <https://doi.org/10.7154/RDG.1995.0009.0004>
- Santos, R. D., Lemos, R. C., Santos, H. G., Ker, J. C., Anjos, L. H. C. (2005). *Manual de descrição e coleta de solos no campo*. 5. ed. Viçosa: SBCS.
- Seo, I. K., Park, Y. S., Kim, N. W., Moon, J. P., Ryu, J. C., Ok, Y. S., Kim, K., Lim, K. J. (2010). Estimation of soil erosion using SATEEC and USPED and determination of soil erosion hot spot watershed. *Journal of Korean Society on Water Quality*, 26(3), 497-506.
- Serviço Geológico do Brasil (CPRM), Coordenadoria de Planejamento Ambiental (CPLA). (2002). *Atlas geoambiental das bacias hidrográficas dos rios Mogi-Guaçu e Pardo – SP: subsídios para o planejamento territorial e gestão ambiental*. São Paulo: CPRM/CPLA. Available at: [https://rigeo.cprm.gov.br/jspui/bitstream/doc/2548/1/Atlas\\_Geoamb\\_Mogi\\_Pardo.pdf](https://rigeo.cprm.gov.br/jspui/bitstream/doc/2548/1/Atlas_Geoamb_Mogi_Pardo.pdf). Accessed on: Jan 17, 2022.
- Silva, A. M., Alvares, C. A. (2005). Levantamento de informações e estruturação de um banco dados sobre a erodibilidade de classes de solos no Estado de São Paulo. *Geociências*, 24(1), 33-41. Available at: <https://ppegeo.igc.usp.br/index.php/GEOSP/article/view/9738>. Accessed on: Jan 17, 2022.
- Silva, D. C. C., Albuquerque Filho, J. L., Sales, J. C. A., Lourenço, R. W. (2017). Identificação de com perda de solo acima do tolerável usando NDVI para o cálculo do fator C da USLE. *Ra'eGa.*, 42, 72-85. <https://doi.org/10.5380/raega.v42i0.45524>
- Silva, R. M., Santos, S. A. G., Montenegro, S. M. G. L. (2013). Identification of critical erosion prone areas and estimation of natural potential for erosion using GIS and remote sensing. *Revista Brasileira de Cartografia*, 65(5), 881-894.
- Sir, B., Bobál, P., Richnavský, J. (2013). GIS evaluation of erosion-sedimentation risk caused by extreme convective rainstorms: case study of the Stonávka River Catchment, Czech Republic. In: J. Kozak, K. Ostapowicz, A. Bytnerowicz, B. Wyzca (Eds.). *The Carpathians: integrating nature and society towards sustainability*, 1, 45-58. Berlin: Springer. [https://doi.org/10.1007/978-3-642-12725-0\\_5](https://doi.org/10.1007/978-3-642-12725-0_5)
- Tamene, L., Vlek, P. L. G. (2008). Soil erosion studies in Northern Ethiopia. In: A. K. Braimoh, P. L. G. Vlek (Eds.). *Land use and soil resources*, 1, 73-100. Berlin: Springer. [https://doi.org/10.1007/978-1-4020-6778-5\\_5](https://doi.org/10.1007/978-1-4020-6778-5_5)
- Tarboton, D. G. (1997). A new method for the determination of flow directions and upslope areas in the grid digital elevation models. *Water Resources Research*, 33(2), 309-319. <https://doi.org/10.1029/96WR03137>
- UCRBEEc. (2010). *Plano de manejo integrado das unidades de conservação reserva biológica e estação ecológica Mogi Guaçu – SP*. Piracicaba: UCRBEEc.
- Warren, S. D., Mitasova, H., Hohmann, M. G., Landsberger, S., Iskander, F. Y., Ruzycski, T. S., Senseman, G. M. (2005). Validation of a 3-D enhancement of the Universal Soil Loss Equation for prediction of soil erosion and sediment deposition. *Catena*, 64(2-3), 281-296. <https://doi.org/10.1016/j.catena.2005.08.010>
- Warren, S. D., Ruzycski, T. S., Vaughan, R., Nissen, P. E. (2019). Validation of the Unit Stream Power Erosion and Deposition (USPED) Model at Yakima Training Center, Washington. *Northwest Science*, 92(Spe. 5), 338-345. <https://doi.org/10.3955/046.092.0504>
- Weill, M. A. M., Rocha, J. V., Lamparelli, R. A. (2001). Potencial natural de erosão e riscos de degradação na bacia hidrográfica do Rio Mogi Guaçu. *VII Simpósio Nacional de Controle de Erosão*. Goiânia. CD-ROM.
- Wischmeier, W. H., Smith, D. D. (1978). *Predicting rainfall erosion losses: a guide to conservation planning*. Washington: USDA. Available at: <https://naldc.nal.usda.gov/download/CAT79706928/PDF>. Accessed on: Jan 17, 2022.